Application of Oscillating Potentials to the Shaker Potassium Channel

A. Kargol[1], A. Hosein-Sooklal[2], L. Constantin[3] and M. Przestalski[4]

[1] *Loyola University, Physics Department, New Orleans, LA 70118, U.S.A.*
[2] *University Of Arkansas for Medical Sciences, Department of Physiology and Biophysics, Little Rock, AR 72205, U.S.A.*
[3] *Tulane University, Physics Department, New Orleans, LA 70118, U.S.A.*
[4] *Medical Academy, Otolaryngology Clinic, 50368 Wrocław, Poland*

Abstract. Nonequilibrium response spectroscopy (NRS) has been proposed recently to complement standard electrophysiological techniques used to investigate ion channels. It involves application of rapidly oscillating potentials that drive the ion channel ensemble far from equilibrium. It is argued that new, so far undiscovered features of ion channel gating kinetics may become apparent under such nonequilibrium conditions. In this paper we explore the possibility of using regular, sinusoidal voltages with the NRS protocols to facilitate Markov model selection for ion channels. As a test case we consider the Shaker potassium channel for which various Markov models have been proposed recently. We concentrate on certain classes of such models and show that while some models might be virtually indistinguishable using standard methods, they show marked differences when driven with an oscillating voltage. Model currents are compared to experimental data obtained for the Shaker K^+ channel expressed in mammalian cells (tsA 201).

Key words: Potassium ion channel — Markov model — Nonequilibrium response spectroscopy

Introduction

Voltage-gated ion channels are transmembrane proteins forming pathways for ion exchange between a cell and the extracellular medium. One of the goals in ion channel studies is to develop kinetic models of their gating. The aim of this paper is to present a new method for verifying kinetic models for various ion channels by studying them under nonequilibrium conditions. The method is tested on the Shaker potassium channel and we show that the use of oscillating potentials in voltage clamp experiments allows one to falsify otherwise indistinguishable models.

Correspondence to: Armin Kargol, Loyola University, Physics Department, New Orleans, LA 70118, U.S.A. E-mail: akargol@loyno.edu

The bulk of experimental data on ion channels comes from electrophysiological studies using voltage clamp techniques (Hille 1992). The technique of voltage clamp since its inception underwent various modifications and improvements, including the patch clamp method (Sakmann and Neher 1995). However, the main idea for all protocols used in published studies has been a stepwise change of transmembrane voltage and observation of channel relaxation to a steady state. Models of various ion channels (Vandenberg and Bezanilla 1991a,b; Hoshi et al. 1994; Zagotta et al. 1994a; Schoppa and Sigworth 1998a,b,c) have been proposed but they are nonunique (Kienker 1989; Schoppa and Sigworth 1998a,b,c; Wagner and Timmer 2000). Typically there are several different models capable of reproducing the experimental data equally well while differing significantly in their properties. This model ambiguity can be at least partially blamed on intrinsic limitations of standard stepped-voltage protocols used in channel electrophysiology.

Recently a novel approach aimed at expanding the range of protocols used in voltage clamp experiments and known as the *nonequilibrium response spectroscopy* (NRS) has been proposed (Millonas and Hanck 1998a,b). It involves applying rapidly fluctuating voltage waveforms instead of stepwise changing voltages. With standard voltage clamp protocols the cell (an ensemble of ion channels) is kept at a holding voltage for a significant period of time. This ensures that the system is in thermodynamical equilibrium at given temperature and for this voltage. To avoid confusion with a notion of equilibrium typically used in thermodynamics we emphasize that we do not mean the equilibrium of solutions on both sides of the membrane (which effectively would mean no ion fluxes and hence no currents), but rather the equilibrium of an ensemble of ion channels as they undergo the gating process influenced by the applied voltage and populate various conformational states. This equilibrium means no net transitions between various configurational states of the channel molecules. When the voltage is changed in a step-like fashion, the state of equilibrium is disturbed. However with time the system equilibrates at a new state corresponding to the new value of the membrane potential. The observed currents (ionic or gating, whole cell or patch) reflect the system's relaxation to the new equilibrium state. If a fluctuating potential is applied instead, the energy can be continuously transferred from the electric field to the channel molecules, hence driving them arbitrarily far from any equilibrium state. In that respect the fluctuating voltages form an entirely new class of experimental protocols.

The ambiguity in channel modeling is not restricted to details within a certain class of models. There is some disagreement about the type of models that best describe the channel kinetics. Although the discrete Markov models (DMMs) are by far the most commonly used, other models have been considered. These alternatives include fractal models, diffusion models, continuum models, etc. (Liebovitch et al. 1987; Levitt 1989; Sansom et al. 1989; Ball and Rice 1992). Published reports argue both in favor (Korn and Horn 1988; McManus et al. 1988) and against (Liebovitch et al. 1987) the use of DMMs. On the other hand the DMM's are approximations valid on a certain time scale only. If the discrete states in DMM reflect minima in the channel molecular "energy landscape" with thermally acti-

vated transitions between the minima, this picture is valid on a time scale longer than the relaxation times for the intra-well configurational changes (Millonas 2000). Nevertheless in this paper we concentrate on the DMMs. As we mentioned they are not only commonly used but to some extent they are rooted in the molecular dynamics.

In this paper we make the case for the use of oscillating potentials in facilitating model selection from among a certain subset of possible Markov models. The technique is not intended to replace, but to complement currently used methods based on whole cell and single-channel recordings. A more general presentation of the NRS technique (Kargol et al. 2002) and first applications to the human heart sodium channel have been published (Millonas and Hanck 1998a,b; Hosein-Sooklal and Kargol 2002). The idea of driving biological macromolecules with oscillating potentials originated with the work of Fohlmeister and Adelman (1985a,b, 1986, 1987) who recorded gating current responses of sodium channels in giant squid axons to sinusoidal voltage stimulus of frequency ranging from 500 Hz to 5 kHz. Their study concentrated on nonlinearities in the channel responses, in particular the higher harmonic content, finding them irreconcilable with kinetic Hodgkin–Huxley type models. More recently a study of periodic forcing of single channels (Menconi et al. 1998) showed the dependence of single channel dwell time and cycle histograms on properties of the driving voltage and other environmental variables (e.g. temperature). Sinusoidal voltage waveforms were also applied to an ion pump, the Na,K-ATPase (Liu et al. 1990; Xie et al. 1997). It has been shown that at low temperatures, when the ATP hydrolysis activity is significantly decreased or with cells pre-treated with ouabain – a known inhibitor – stimulation of the cell with high frequency regular (sinusoidal) voltages produced a unidirectional ionic flow measured by radioactive tracers. The Na and K pumping modes were activated independently at different frequencies. It has been concluded that the enzyme must be able to absorb energy from the electric field and convert it into chemical potential energy of an ion. A four-state transport model has been proposed and the effect of the electric field included by means of electroconformational coupling.

We use the Shaker potassium channel as a test case for the nonequilibrium study. It is one of the best known and most extensively studied voltage-gated ion channels. The channel is a tetramer of subunits with six membrane-spanning segments each. The structure of the channel has been determined with X-ray crystallographic methods (Jiang et al. 2003a). Despite this, little is known about details of molecular motions underlying channel kinetic features, such as voltage sensing, gating or selectivity. The S4 segment, containing charged residues, has been long postulated to be the molecular voltage sensor with the measured gating currents reflecting the movement of these residues as the molecule underwent conformational changes. Molecular motion of the S4 segment was postulated to be a screw-like turn and transverse shift (Hille 1992). Recent studies suggest more complex motions: voltage-sensor paddles (Jiang et al. 2003b) proposed from a combination of biochemical, X-ray crystallographic and electrophysiological measurements; the evidence of a tilt in the S4 position obtained by measuring distances between various

locations on S4 segments with fluorescence resonance energy transfer (FRET or LRET) (Cha et al. 1999; Glauner et al. 1999; Bezanilla 2002). Coupling of the voltage sensor to the activation gate (the S6 segment) has also been investigated pointing to an important role of the S4-S5 linker (Larsson 2003). These results are first direct observations of the molecular structure and conformational changes of the channel molecules during gating. On the other hand there are detailed functional studies based on electrophysiological measurements, that led to the development of kinetic models of channel gating. The kinetic models include known features of channel structure, such as the four-fold symmetry, or the existence of the intermediate positions of the voltage sensor (Gandhi and Isacoff 2002). Out of several kinetic studies of Shaker channel (Vandenberg and Bezanilla 1991a,b; Schoppa and Sigworth 1998a,b,c) we concentrate here on (Hoshi et al. 1994; Zagotta et al. 1994a,b). In a series of three papers several classes of Markov models have been proposed. They are based on all types of currently available electrophysiological data, including whole cell ionic, gating and single channel currents. In this paper we revisit the models and investigate their behavior in response to oscillatory voltage stimulus used in a standard voltage clamp experiment.

Materials and Methods

Cell culture and channel expression

We studied a mutant Shaker channel (Shaker K Sk1) with the fast inactivation removed. The channels were stably expressed in tsA 201 cells (a gift of D. Hanck) maintained in Dulbecco's modified eagle medium (DMEM) (Gibco BRL, Gaithersburg, MD, U.S.A.) supplemented with 10% fetal bovine serum (Gibco BRL), 1% penicillin/streptomycin (Cellgro, Herndon, VA, U.S.A.) and 200 μg/ml Zeocin (Invitrogen, Carlsbad, CA, U.S.A.) at 37° in 5% CO_2. The cells were grown in 35 mm Corning dishes and released with 250 μl of trypsin w/EDTA (Cellgro).

Recording apparatus

We used a typical whole-cell recording setup for ionic currents. The setup consisted of the Axopatch 200B amplifier with a CV 203 BU headstage (Axon Instruments Inc., Union City, CA, U.S.A.) and the Axiovert inverted microscope (Carl Zeiss Inc., Thornwood, NY, U.S.A.). The voltage protocols were either read from binary files generated by Matlab (Mathworks Inc., Natick, MA, U.S.A.) programs (oscillatory voltages) or prepared using a template (stepped-voltage protocols) in a Pulse program (Heka Electronik GmbH, Lambrecht, Germany) running on a Pentium III 450 MHz Gateway computer (Gateway Inc., San Diego, CA, U.S.A.). The data was filtered at 10 kHz on an analog filter, digitized at 200 kHz using the ITC18 AD/DA converter (Instrutech Corp., Great Neck, NJ, U.S.A.) and stored on a disk.

The main concern in the experimental apparatus set up was the recording bandwidth that would allow application of oscillatory voltage waveforms with sufficiently high frequencies. A version of balloon pipettes described previously (Millonas and Hanck 1998a) were made from borosilicate glass on a Sutter pipette

puller (SDR Clinical Technology, Middle Cove, NSW, Australia). The pipette resistance typically varied around 600–800 kΩ. We used a Soma micromanipulator (Soma Scientific, Irvine, CA, U.S.A.) and a Physitemp temperature control system (Physitemp Instruments Inc, Clifton, NJ, U.S.A.). All experiments were performed at 12 ℃.

Seals in excess of 1 GΩ were routinely obtained. Data presented here were collected from cells for which input RC time did not exceed 20 μs, which corresponds to 8 kHz recording bandwidth. If needed the bandwidth could be further increased using the soft glass balloon pipettes (Millonas and Hanck 1998a). Series resistance compensation was not used.

Solutions

The extracellular solution was (in mmol/l): 140 NaCl, 4 KCl, 2 $CaCl_2$, 1 $MgCl_2$, 10 HEPES (pH 7.4) and the intracellular solution was: 130 KCl, 10 NaCl, 2 $MgCl_2$, 1 $CaCl_2$, 11 EGTA, 10 HEPES (pH 7.4). Both were filtered through 20 μm filter before use.

Pulse protocols

For the standard activation series the cells were held at −70 mV until a voltage step to a series of depolarized voltages from −70 mV to 42 mV in 8 mV increments. The tail currents were recorded by depolarizing the cell to 30 mV for 20 ms followed by repolarization to potentials from −170 mV to 10 mV in steps of 12 mV. For both protocols the leak currents and capacity transients were subtracted using the standard P/4 method (Bezanilla and Armstrong 1977) with potentials not exceeding −90 mV. The protocols were prepared from a template in Pulse program (see Recording apparatus).

The oscillatory protocols involved a series of sine functions with variable amplitude and frequency. The cells were held at the same voltage of −90 mV until an oscillatory pulse with a chosen amplitude, mean value and the frequency was applied. We tested four sine wave amplitudes (15, 30, 45 and 60 mV), four mean values (−45, −30, −15 and 0 mV) and frequencies varying from 100 Hz to 4 kHz. The P/4 method was used with all sine protocols. The pulses were created using Matlab programs and stored on a hard disk as floating-point number files. The voltage sampling rate for all protocols was 10 μs.

Data analysis and model fitting

All data analysis programs were written in Matlab. The experimental data was stored on a disk as a binary file.

Cell properties

As we mentioned one of the critical conditions for our recording apparatus is a sufficiently high bandwidth. The RC time was determined from capacity transients recorded in response to a voltage step. Only records with the time constant not exceeding 20 μs (corresponding to 8 kHz bandwidth) were kept. In addition the cell

capacitance was determined by integrating capacity transients elicited in response to a series of voltage steps from the holding potential of −130 mV to a series of voltages not exceeding −90 mV.

Ionic currents

An activation curve was determined from the activation series by estimating the stationary current for each voltage step. An instantaneous current-voltage relationship was obtained from the tail series by measuring the maximum current at certain short time interval after the membrane repolarization (typically 100–150 μs). The reversal potential was computed by fitting the instantaneous i-V relationship.

Model fitting

The experimental data (the activation series and the tail currents) were used to find, within a certain class, models capable of reproducing the data to certain accuracy. Details of models analyzed here are given in the Theory section below. Although in our study the model parameters for each of the class of the models shown in Fig. 1 were determined by fitting the activation and tail currents only, we stress that the model topologies we used and which were developed in (Hoshi et al. 1994; Zagotta et al. 1994a,b) fit ionic, gating *and* single channel recordings.

For each of the models the values of model parameters (rate constants) were determined with the help of a simulating annealing algorithm described earlier (Millonas and Hanck 1998a). The algorithm is a random search in a parameter space with decreasing search range. We start with a randomly chosen model (a set of parameters). For every generation we generate a number of new models from the original one by randomly perturbing the values of parameters within certain, decreasing, range. We then select the best model based on the fit to experimental data and this model becomes a "parent" for the next generation. The accuracy of the model fit was determined by the χ^2 error. Typically each run consisted of 2000 generations and took from 2–10 h on a Pentium III 450 MHz PC, depending on the size of the model.

We computed the model current that can be directly compared to experimental data as follows

$$i(t) = g_0 g(V)(V - V_r)\boldsymbol{O} \cdot \boldsymbol{P}(\boldsymbol{t}) \tag{1}$$

where $\boldsymbol{P}(t)$ denotes the time dependent probability vector (see Theory) and $\boldsymbol{O}$ is the projection vector onto open states, so that $\boldsymbol{O}\cdot\boldsymbol{P}(t)$ is the total probability of the channel being open. V_r is the reversal potential determined from the instantaneous current-voltage relationship as described above. $g(V)$ represents nonlinear terms in instantaneous conductance and has to be determined from experimental data. In many reported studies little attention is paid to this term and frequently model currents are individually scaled to match experimental activation and tail data (Zagotta et al. 1994a,b). That corresponds to computing $g(V)$ at discrete voltages only. In our case since we apply smoothly varying voltages we need a functional form of $g(V)$. We obtained it by fitting the discrete values of $g(V)$ with a third or

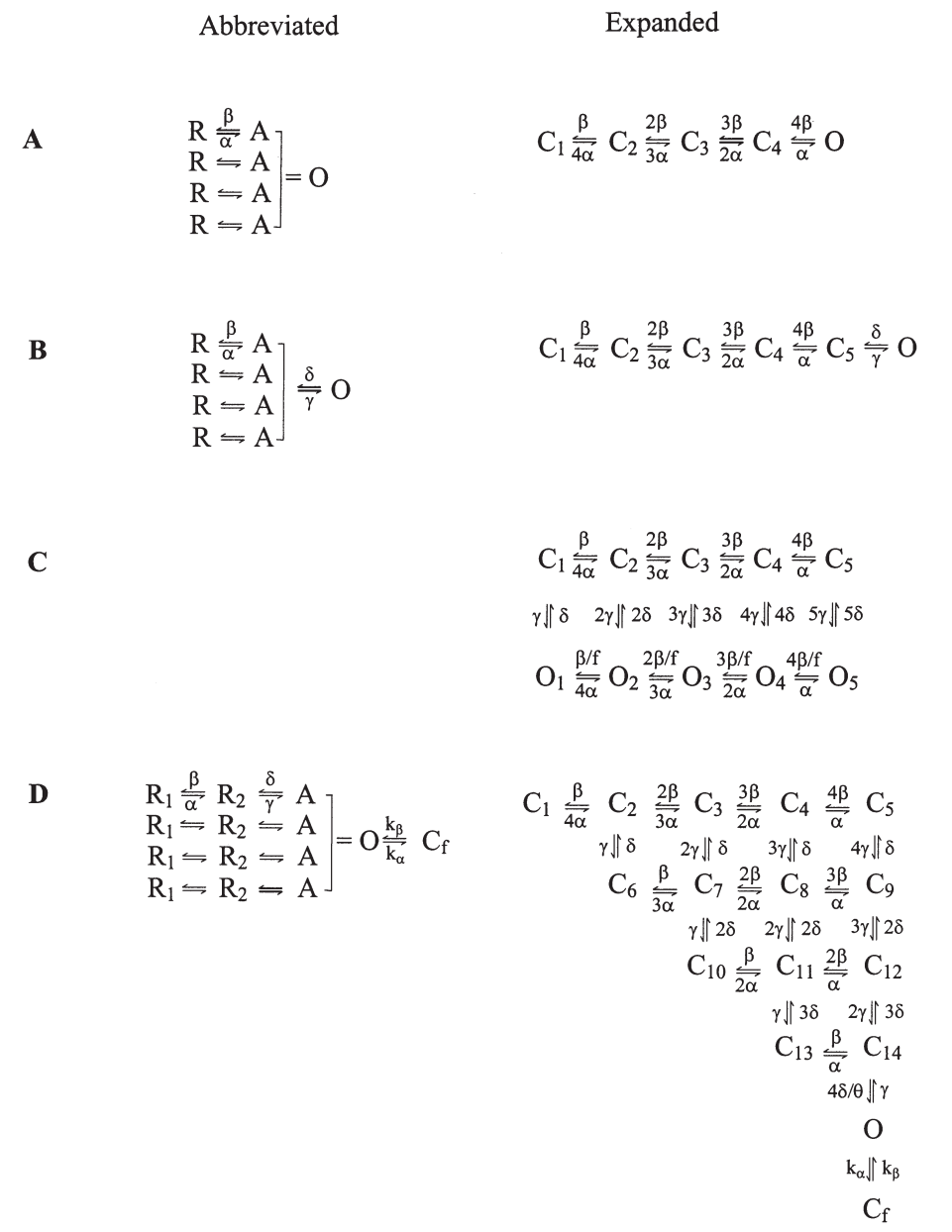

Figure 1. Markov models for the Shaker K^+ channel proposed in Zagotta et al. (1994a). In the abbreviated form the models show fourfold symmetry derived from the primary structure of the channel molecule. Each of the S4 segments undergoes one or two independent transitions. In the expanded form the transition rates are expressed in terms of the rates for single S4 segment transitions.

fifth order polynomial. We emphasize that this was done only once for any given cell and then the same conductance function was used for all models tested. g_0 is an overall scaling factor representing the cell expression rate (the overall number of channels in the cells) and was typically included as one additional parameter in the optimization algorithm.

Theory

Overview of discrete Markov models

Observable ion channel gating is believed to be the result of conformational changes of the channel molecule in response to environmental factors (like the membrane potential in the case of voltage gated channels). The channel protein has at least two (typically more) meta-stable conformational states corresponding to closed and open channels. From a physical viewpoint conformational changes of the molecule are represented by its energy and the stable states reflect the energy minima. Markov models of channel kinetics assume the channel has only a number of discrete states, in other words it disregards the shape of each energy well and all possible relaxation effects occurring within the well. Transitions between the Markov states correspond then to thermally activated "jumps" over potential barriers separating neighboring wells. This picture of ion channel kinetics, however simplified, has been useful in explaining and categorizing experimental data. Our goal here is to improve model selection and parameter estimation, remaining, however, within this class of models.

Typically DMMs are described as a kinetic scheme (a set of states connected by possible transitions – referred to as the model topology) and the transition rates. Kinetic schemes of the DMMs considered here are given in the following section. For each of the models the transition rates are assumed to have the standard Eyring form (Eyring 1935)

$$\begin{aligned} \alpha_i(V) &= \alpha_i(0)\exp(q_i^+ V/kT) \\ \beta_i(V) &= \beta_i(0)\exp(q_i^- V/kT) \end{aligned} \tag{2}$$

where $q_i^{\pm}$ are the gating charges associated with each forward (resp. backward) transition. The gating charges as well as parameters $\alpha_i(0)$ and $\beta_i(0)$ are exactly the set of parameters that need to be determined (in addition to model topology) by fitting the experimental data in order to specify the model for a channel. For each model the time course of the open probability is obtained by projecting the probability vector $\boldsymbol{P}(t)$ (the vector of probabilities for the channel being in each of the states of the model) onto the open state(s). The probability vector satisfies the master equation

$$\frac{\mathrm{d}\boldsymbol{P}(t)}{\mathrm{d}t} = \mathbf{W}\boldsymbol{P}(t) \tag{3}$$

subject to initial condition $\boldsymbol{P}(0) = \boldsymbol{P}_{\mathbf{o}}$. $\mathbf{W}$ denotes the transition matrix for each particular Markov model. For stepped voltage protocols the matrix $\mathbf{W}$ is independent of time (with the exception of the step time when it changes from on value to

another). Then the solution to the master equation has a form

$$\boldsymbol{P}(t) = \exp(\mathbf{W}t)\boldsymbol{P_o} \tag{4}$$

which can be computed using standard matrix routines from Matlab. For time-varying potentials the matrix $\mathbf{W}$ becomes time dependent itself (through the dependence of the transition rates α_i and β_i on the voltage) and a formal solution to Eq. (3) can be written as

$$\boldsymbol{P}(t) = \exp\left(\int_0^t \mathbf{W}(s)\mathrm{d}s\right)\boldsymbol{P_o} \tag{5}$$

We find explicit form of a solution to Eq. (4) by iteration with a suitable time step, typically equal to the sampling rate

$$\boldsymbol{P}(t_{i+1}) = \exp(\mathbf{W}t_i)\boldsymbol{P}(t_i) \tag{6}$$

The choice of initial probability vector $\boldsymbol{P_o}$ depends on the experimental protocols we are trying to model. Typically, prior to application of a specific voltage pulse the system is kept at the "holding" potential for a significant period of time. For computational purposes $\boldsymbol{P_o}$ was in each case determined by solving the master Eq. (3) with the transition matrix corresponding to the holding potential and sufficiently long t to ensure full equilibration at this voltage.

Shaker K^+ channel models

We concentrate on models proposed in Zagotta et al. (1994a) further reffered to as ZHA models. A very detailed analysis of the models in terms of their response to stepped voltage protocols has been presented (Hoshi et al. 1994; Zagotta et al. 1994a,b). The models developed there all are compatible with the experimental data in a form of whole-cell ionic and gating currents as well as single channel data. The kinetic schemes for all models are reproduced in Fig. 1. Model A, the simplest of the four, has four independent transitions corresponding to each of the S4 segments moving independently. Once all four are in the activated position, which occurs after only one transition *per* segment, the channel as a whole opens. Henceforth, the model when shown in a fully expanded version has only two independent transition rates, which corresponds to four model parameters (the rate amplitudes and gating charges). Models of class B have one additional feature – the channel opening occurs following an additional transition from a state with all four S4 segments activated. Since that additional transition is independent from the S4 activation, there are 4 transition rates (8 model parameters) to be found. Models of class C, on the other hand, assume that a channel is open even when only one of the S4 segments activates. This opening transition ($C_i \rightarrow O_i$) is, however, stabilized by the S4 segments activation. This is expressed by a factor f in the overall transition rates. In the original form the model was presented with equilibrium rates, but in Fig. 1 we show a particular form of transition rates we assumed.

Moreover, the opening transition is assumed voltage independent and hence we might expect a small nonzero current at all voltages, even hyperpolarized. Class D models have two modifications. First, it is assumed that not one, but two independent transitions are needed for each S4 segment to reach an activated state, and second, an inactivated state, reachable only after passing through the open state is assumed. Since the S4 transitions are identical, there are 6 different transition rates (12 model parameters). These various properties of the models proposed were introduced in (Hoshi et al. 1994; Zagotta et al. 1994a,b) to account for different features in measured ionic and single channel experimental data.

Of course other models, typically more complex, have been proposed by other authors, but here we intend to compare nonequilibrium responses of only those four simplest cases.

Results

Activation and tail protocols

We used models developed in (Hoshi et al. 1994; Zagotta et al. 1994a,b), however, we first recorded our own data for standard protocols and reoptimized ZHA models to fit our data. Channel activation series is typically one of the basic types of data recorded from ion channels and used for model development. The cells were held at a potential of -70 mV and then the membrane was depolarized to a series of voltages from -70 to $+42$ mV. The data were leak and capacity corrected as described in Materials and Methods. Sample currents are shown in Fig. 2A. We estimated the stationary state (at $t > 50$ ms) and plotted against the depolarized voltage in Fig. 2B. Data shown is from a cell with capacitance 27.25 μF and RC time of 20 μs.

Tail currents were taken for steps from a depolarized voltage of 30 mV to a series of values from -110 to -2 mV in -12 mV steps (Fig. 3A). The instantaneous current voltage relationship (Fig. 3B) was obtained by plotting tail currents at a fixed time (of the order of 100 μs after the re-polarization step) as a function of voltage. This instantaneous i-V plot was used to determine the nonlinear conductance $g(V)$. Since the current is measured shortly after the re-polarization step, the open probability is still almost unchanged (from its value at the prepulse) and is the same for all repolarizing voltages. Hence the instantaneous current should be proportional to $(V - V_r)$. Any deviation from linearity can be included in $g(V)$ and attributed to effects other than channel kinetics and therefore independent of any particular model of channel gating. Once fixed $g(V)$ was unchanged for the rest of simulations and was the same for all models considered. Fig. 3B shows the instantaneous i-V relationship (the dots) and the solid line is the current computed with $g(V)$ fitted by a 3rd order polynomial.

Fig. 2C shows the effective membrane conductance including both the nonlinear effects and the channel gating effects. In Fig. 2D the nonlinear conductance effects were taken into account and only the kinetic effects are plotted. The graph

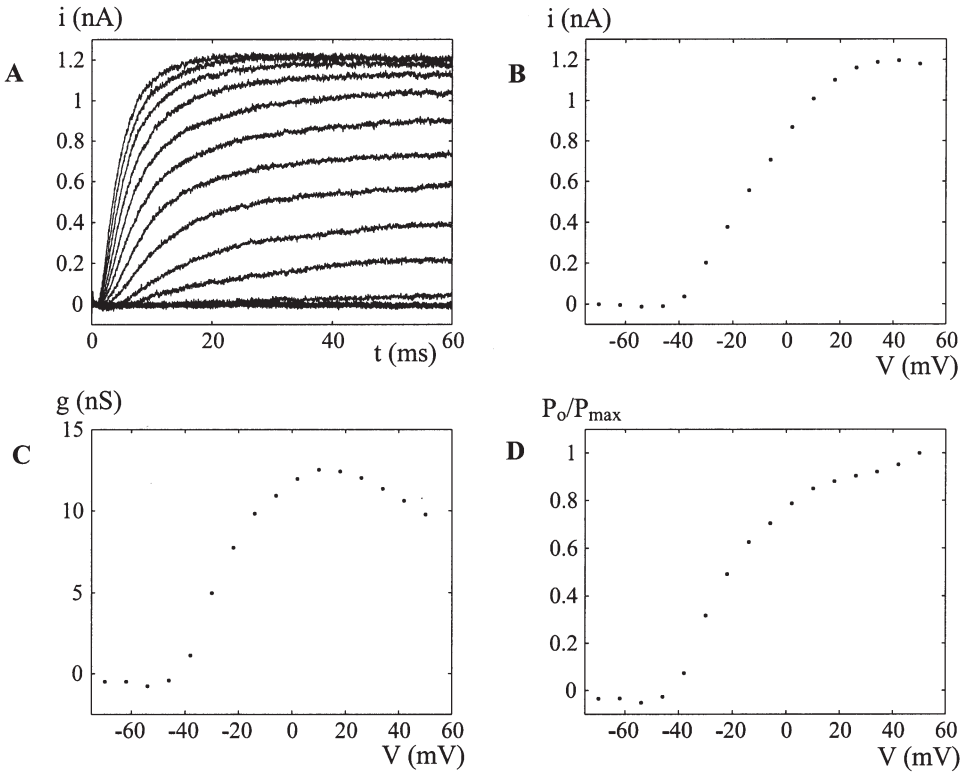

Figure 2. Activation series. A. Current transients obtained for voltage steps from the holding potentials of −70 mV to a series of voltages from −70 to +42 mV in 8 mV steps. Data were filtered at 10 kHz on an analog filter and capacity and leak corrected with the P/4 method. B. Activation curve. The steady state current recorded at $t >$ 50 μs as a function of membrane potential. C. Membrane conductance obtained from the activation curve (Fig. 2B) and Eq. (1). D. Membrane conductance after taking into account nonlinear effects. The nonlinear part of the conductance $g(V)$ was obtained from the tail instantaneous i-V relationship (Fig. 3B) and fit with a 3rd order polynomial. The curve is normalized to the maximum value.

shows the activation degree (the open probability relative to the maximal open probability) in response to depolarization steps.

Model fitting

Both activation and tail currents were used to determine model parameters as described in Materials and Methods. The nonlinear conductance $g(V)$ used was the same for all models, but the overall scaling factor g_0 was independently adjusted for all models as a part of the optimization algorithm. Fig. 4 shows fits to activation current traces for four classes of models considered. While models A, B, and D

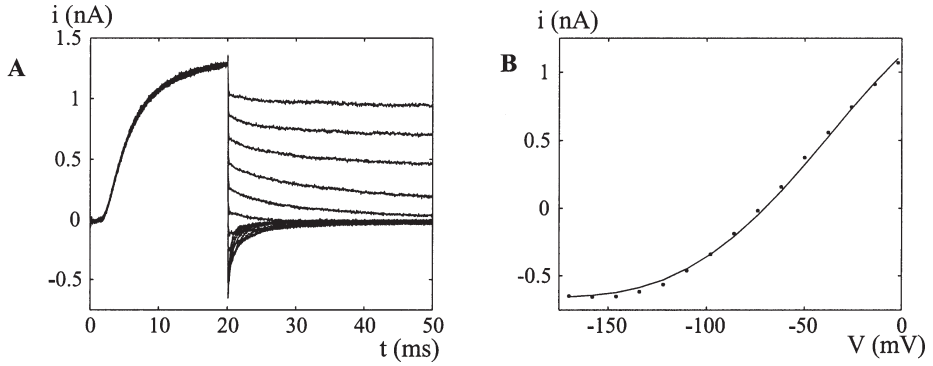

Figure 3. Tail data. A. Current transients obtained for voltage steps from a prepulse of 30 mV to a series of values between −110 and −2 mV in 12 mV steps. Capacity and leak correction as for the activation current traces. B. The instantaneous i-V relationship. The current transients were observed to settle to their maximum values after 50–100 μs. The current values at 100 μs were plotted against voltage. The solid line is a polynomial fit to the nonlinear conductance $g(V)$.

Table 1. Model parameters

Model	Rate amplitudes (s^{-1})	Gating charges (units of e)	Additional parameters	Fitting accuracy (nA^2)
A	$\alpha(0) = 124.8$	$q_\alpha = 0.66$	$g_0 = 1.013$	0.0034
	$\beta(0) = 4.74$	$q_\beta = -0.64$		
B	$\alpha(0) = 864.4$	$q_\alpha = 0.36$	$g_0 = 1.013$	0.002
	$\beta(0) = 32.4$	$q_\beta = -1.51$		
	$\gamma(0) = 101.6$	$q_\gamma = 0.54$		
	$\delta(0) = 13.6$	$q_\delta = -0.69$		
C	$\alpha(0) = 54.0$	$q_\alpha = 1.03$	$f = 130880$	0.0123
	$\beta(0) = 3.14$	$q_\beta = -2.2$	$g_0 = 681$	
	$\gamma(0) = 0.85$	$q_\gamma = 0$		
	$\delta(0) = 121$	$q_\delta = 0$		
D	$\alpha(0) = 775.5$	$q_\alpha = 0.155$	$g_0 = 1.0957$	0.0023
	$\beta(0) = 1422.2$	$q_\beta = -0.147$	$\theta = 41$	
	$\gamma(0) = 1100.4$	$q_\gamma = 0.140$		
	$\delta(0) = 264$	$q_\delta = -0.585$		
	$k_\alpha(0) = 289$	$q_{k\alpha} = 0.00517$		
	$k_\beta(0) = 3991$	$q_{k\beta} = -0.257$		

show quite satisfactory fits, particularly models B and D, for model C we notice a unique feature. Since the concerted transition leading from the activated stated of the S4 subunits to the open state of the channel does not require all four S4

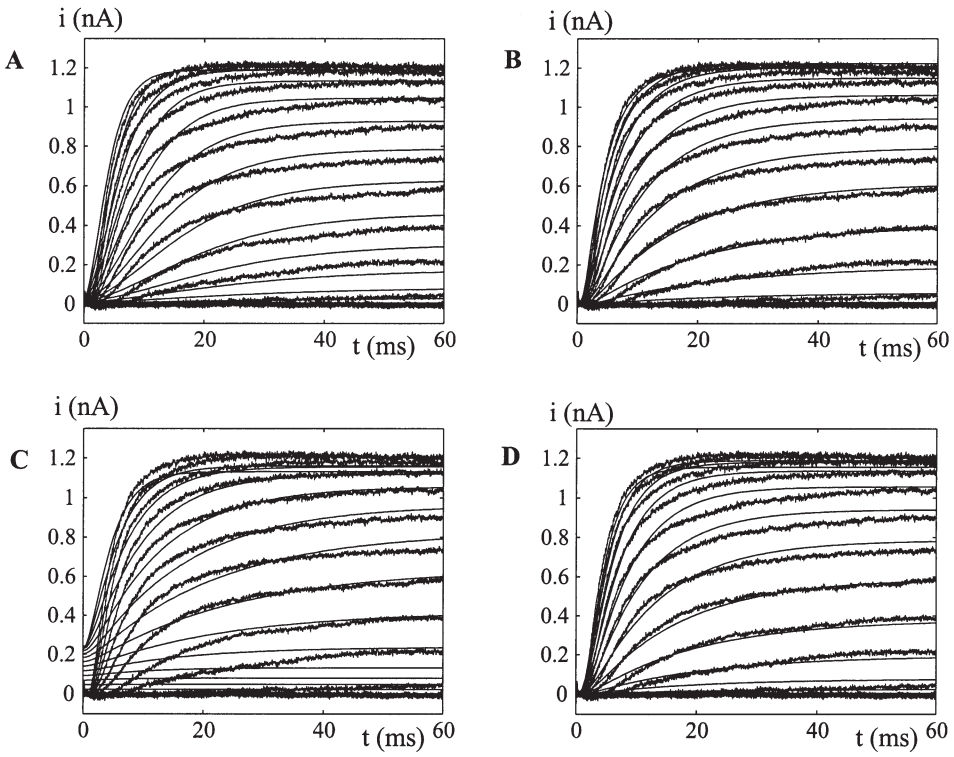

Figure 4. Comparison of model fits to the activation transients. Each plot is one of the four models considered (Fig. 1). Models B and D are able to reproduce experimental data with the same degree of accuracy. Model A is a good qualitative fit, while model C fails at the onset of activation. The voltage independent transition to the open state (see Scheme C in Fig. 1) yields nonzero currents at all voltages. Fitting accuracy as measured by χ^2 normalized to the number of traces and sampling points (Eq. (6)) was 0.0034, 0.0020, 0.0123 and 0.0023 for models A, B, C and D, respectively. Similar fitting accuracy was obtained for the tail current transients.

segments to be activated but is only promoted by these (Zagotta et al. 1994a) and the concerted transition is voltage-independent, one might expect a small current at all voltages, even hyperpolarized. Hence the model is capable of reproducing stationary currents but fails at the onset of activation.

Table 1 shows parameter values obtained for all four models considered. In all cases (with the exception of the activation onset for model C) there is a fairly good fit to experimental data. It is therefore clear from Fig. 4, model fits to tail currents (not shown) and data from Table 1 that our experimental data obtained for stepped voltage protocols are consistent with conclusions reached in (Zagotta et al. 1994a). Model C inadequately reproduces the activation time course, but the selection of

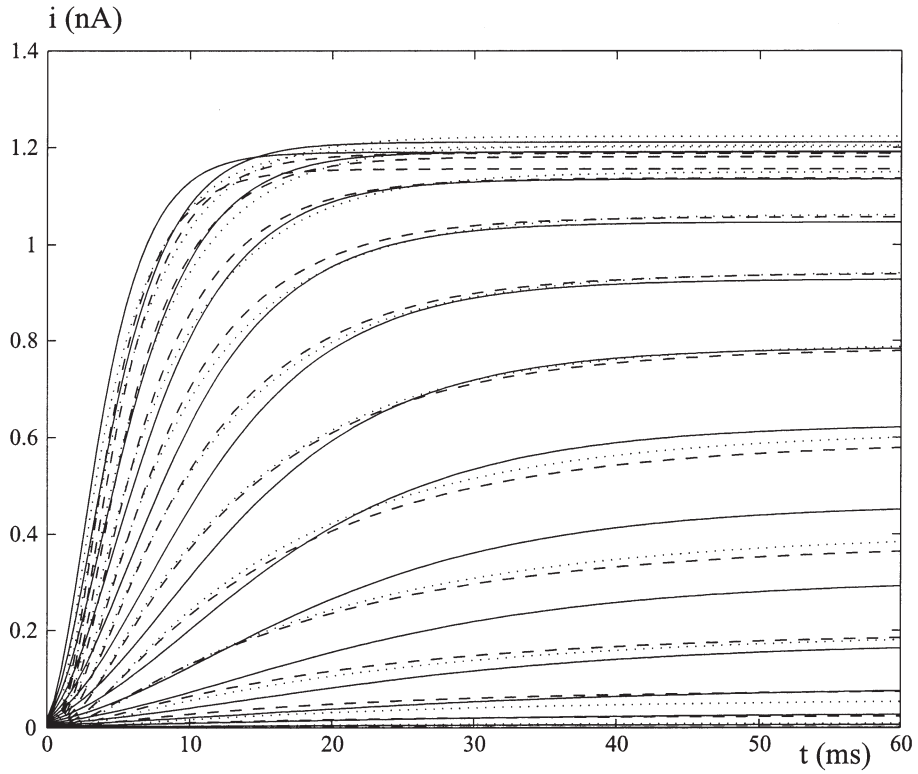

Figure 5. Comparison of model currents predicted by model A (solid line), B (dotted line), and D (dashed line). The currents were computed for the same set of voltage steps as used in experimental protocols (see Fig. 2) using Eq. (1). Model parameters are given in Table 1. The same functional form of nonlinear conductance obtained from the instantaneous current-voltage relationship, as described in text, was used for all three models. The difference among the models was quantified by means of the χ^2 error normalized to number of traces and data points. The difference between models A and B was $\chi^2_{\mathrm{AB}} = 0.0015$, and between B and D the difference was $\chi^2_{\mathrm{BD}} = 0.00032$.

the best of the remaining three models (A, B, and D) is far less certain. To illustrate the point we overlaid the three model currents corresponding to activation protocols in Fig. 5. The voltage steps were the same as for the experimental protocols. Models B and D are virtually indistinguishable and while model A shows a slightly larger deviation from the others both in terms of the activation current sigmoidicity and the stationary values, when measurement errors and noise are taken into account the choice of the best fitting model is uncertain. The model fit to experimental data is quantified in Table 1 where the χ^2 error between the model currents and experimental data is shown. In order to facilitate comparison of different sets of current traces possibly of different duration the χ^2 error was normalized to the

number of traces and the sampling rate

$$\chi^2 = \frac{\sum (I_{\text{exp}} - I_{\text{model}})^2}{\#\text{traces } \#\text{sampling points}} \tag{7}$$

For comparison the overall differences between models A and B as well as B and D were computed the same way. For models A and B the error was $\chi^2_{AB} = 0.0015$ and for models B and D the error was $\chi^2_{\text{BD}} = 0.00032$. This is of the same order of magnitude (case A, B) or even an order of magnitude smaller (case B, D) than the error of fit to experimental data as shown in Table 1. That clearly supports our claim that neither of the models can be selected based on the data.

As we see, the experimental data, although sufficient to produce gating kinetic model(s) including models developed in previous studies, is clearly compatible with many different models, not only in terms of parameter values, but even the overall model topology. In the original paper (Zagotta et al. 1994a) in which the models have been proposed, a very detailed analysis including other types of data has been performed. It included other types of stepped-voltage protocols (different from the activation and tail protocols described above), gating currents and single-channel recordings. This led to a conclusion that class D model with an addition of an inactivated state (such as we used in our modeling) accounts for most of channel behavior. Even so they admit some of the channel features are reproduced better than others. Our goal is to show that models A, B, D considered here can behave very differently under oscillatory driving potential. One possible application of this phenomenon is more efficient model falsification. These oscillatory voltage protocols are not intended to replace but to complement existing techniques.

Model responses to oscillating potentials

Since as we noted, model C is incompatible even with the typical activation data we will not consider it any further. As for the other three we compute the currents elicited in response to oscillating potentials using model parameters obtained in the preceding section. We use here the same voltage waveforms as described in the methods section. For each model the current was computed from Eq. (1) where the open probability $\boldsymbol{P}(t)$ was obtained by iterating Eq. (6) with a time step equal 5 μs. Typically the current had an oscillating (although asymmetrical) form with a varying amplitude where the exact shape depended on the voltage frequency, mean value and amplitude. Fig. 6 shows a sample current computed for model B with the voltage of frequency 1 kHz, mean value 0 mV and the amplitude 45 mV. For visualization purposes we compare only the current envelope (the maximal and minimal values of the current for each cycle). In Figs. 7 and 8 the current envelopes for all three models are compared for two frequencies 0.1 kHz and 1 kHz. In both cases the voltage amplitude was 45 mV and the mean value varied between -45 mV and 0 mV. The solid line represents model A, the dotted line is model B and the dashed line shows model D. For slow oscillations the models have very similar current responses, as we expect from comparison of their activation and

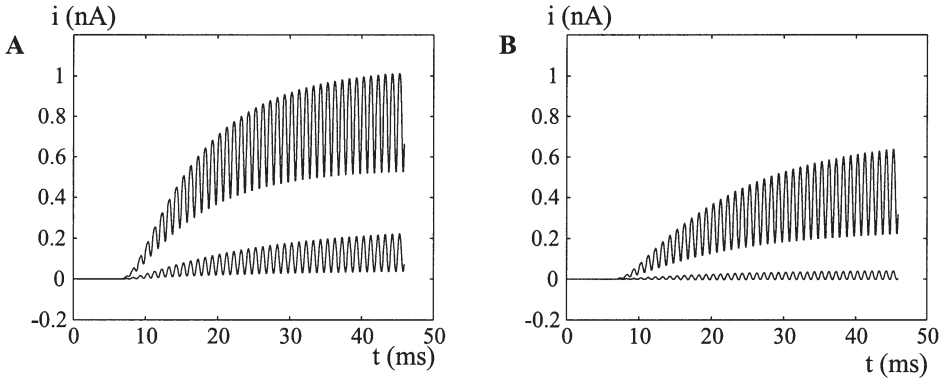

Figure 6. Sample model responses to sinusoidal voltage. The voltage amplitude was 45 mV (90 mV peak-to-peak), frequency 1 kHz, and the mean values: A. 0 mV and −30 mV, B. −15 mV and −45 mV. The currents were computed from Eq. (5) for model D using parameter values shown in Table 1.

tail currents. A significant difference appears for frequency of 1 kHz (or higher). Model A differs significantly from the other two and depending on the mean value of the voltage waveform a difference between models B and D can also be observed. This can be also seen in Fig. 9. It shows the overall difference between models A, B (Fig. 9A) and B, D (Fig. 9B) (measured as the χ^2 error, as described, above) normalized to the corresponding error for stepped voltage protocols. Clearly for low frequencies (< 0.5 kHz) the difference between any of the models is not bigger than the one observed for standard stepped voltage protocols. However, depending on (Zagotta et al. 1994a) the mean value, for higher frequencies the difference computed for oscillating potentials can be 30 (case B, D) or even 45 (case A, B) times larger than observed for stepped voltages. The numerical results just described clearly suggest that such sets of sinusoidal voltages could be used to distinguish between the models.

Experimental responses

Currents were measured for the oscillatory potentials as described in Materials and Methods. The data were capacity corrected using P/4 method. Figs. 7 and 8 show sample traces for frequencies of 0.1 and 1 kHz and mean values of −45, −30, −15 and 0 mV. The experimental data is compared to the model currents represented by their envelopes, as explained in the preceding section. This gives us a direct method for selection of a model most comparable with the experimental data. In Fig. 7 we see that all three models are equally good, or in certain cases model A shows the worst fit. Quantitatively though, the errors of fit to experimental data computed for all three models are of the same order of magnitude as in the case of stepped voltages. That is not surprising since as we commented before the essence of the traditional protocols is to observe the relaxation to a steady state after a

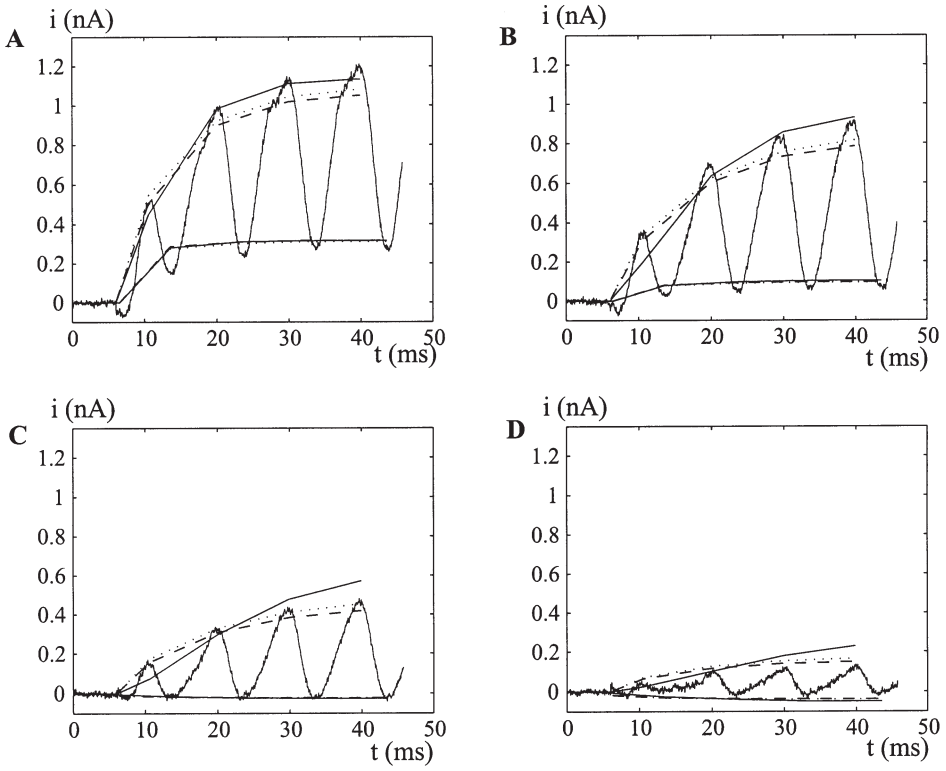

Figure 7. Experimental currents obtained for sinusoidal voltage input. Data recorded from a cell with RC time of less than 20 μs (recording bandwidth 8 kHz). The voltage frequency was 100 Hz, amplitude 45 mV (90 mV peak-to-peak) and the mean values: A. 0 mV, B. −15 mV, C. −30 mV, D. −45 mV. The traces are compared to model currents computed for model A (solid line), model B (dotted line) and model D (dashed line) using parameters from Table 1 and taking into account the nonlinear conductance effects as described in text. For visualization purposes only the current envelopes (the maximal and minimal values of the current in each cycle) are shown.

brief disturbance of the equilibrium. For slow oscillatory potentials the ensemble of channels can be thought of as being in a quasi-steady state – a state where the channel kinetics is faster than the rate of variation of external parameters (in our case the membrane potential) and henceforth the channels remain close to the equilibrium state as this state slowly varies due to the change in membrane potential. Obviously models that performed well for steady states would do equally well in the case of quasi-steady states. From a physical perspective the *adiabatic* approximation is appropriate to describe the ensemble.

The case is quite different for higher frequencies – when the oscillations in the membrane potential become comparable with the natural time scales of the channel

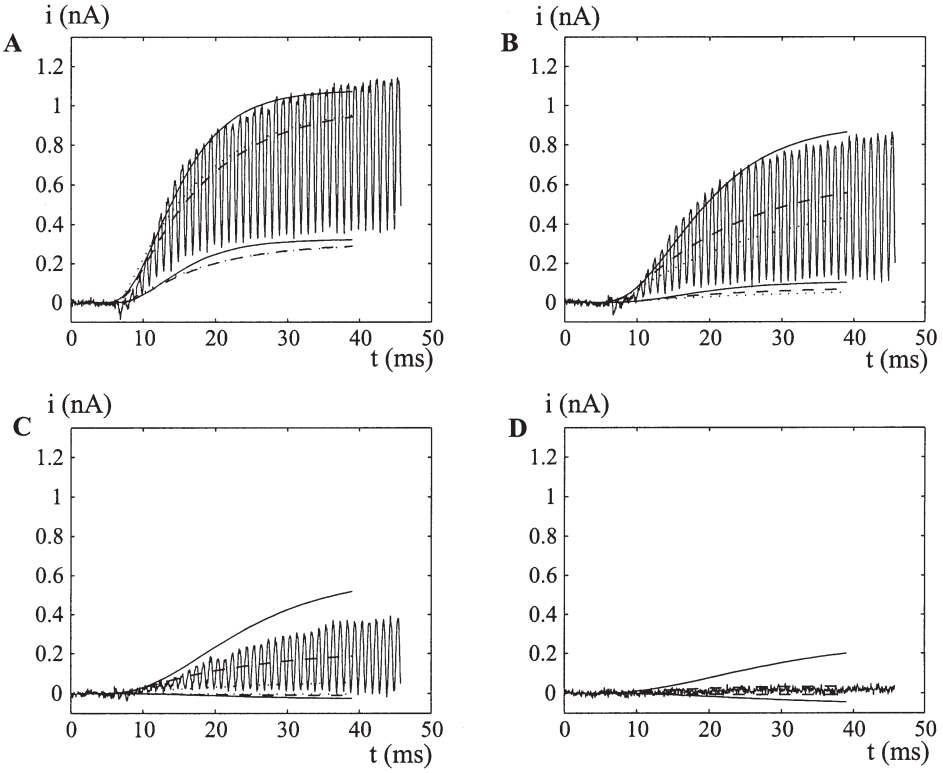

Figure 8. Experimental currents obtained for sinusoidal voltage input. Values the same as in Fig. 7, except for the sine frequency equal 1 kHz.

kinetics. This is illustrated in Fig. 8. There is a much bigger difference between models D (or B) and the experimental data. Again the χ^2 error was computed and it becomes up to 45 (model B) or about 20 (model D) times larger than analogous error for standard stepped-voltage protocols. Fig. 10B shows the difference between model B and the experimental data for the range of frequencies and mean values. Data shown is for the voltage oscillations of amplitude 45 mV, however similar effects were observed for other measured currents (for voltage amplitudes of 15, 30, and especially for 60 mV).

On the other hand, model A seems to perform surprisingly well for higher frequencies. It is visually obvious in Fig. 8 and we verified it quantitatively. The error between model A currents and the experimental data were of the same order of magnitude as the error for stepped voltage protocols. As shown in Fig. 10A for a range of frequencies and mean values of the input sine voltages the overall error between the model (A) and experimental currents is comparable to the error for stepped voltages.

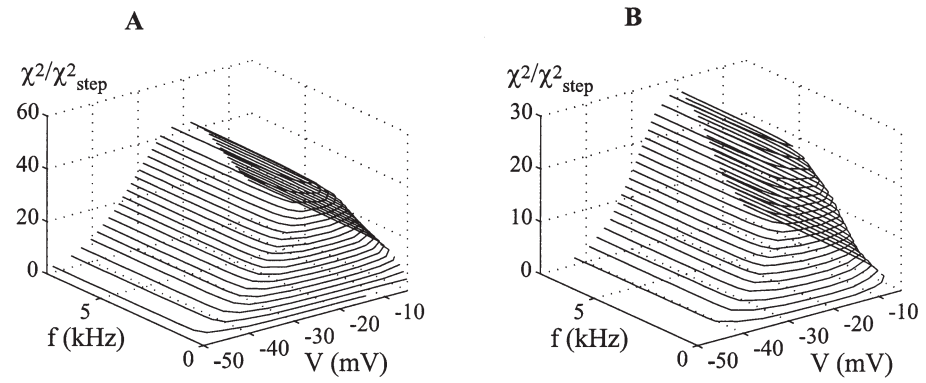

Figure 9. Comparison of model currents obtained for a range of sine voltage inputs varying in frequency (f) and voltage mean value (V). For the voltage amplitude of 45 mV, frequency from 0 to 8 kHz and mean values ranging from −50 to 0 mV, the difference between currents predicted by A. models A, B, and B. models B and D is plotted. The values are scaled to the χ^2_{step} obtained for the stepped-voltage protocols (Fig. 5).

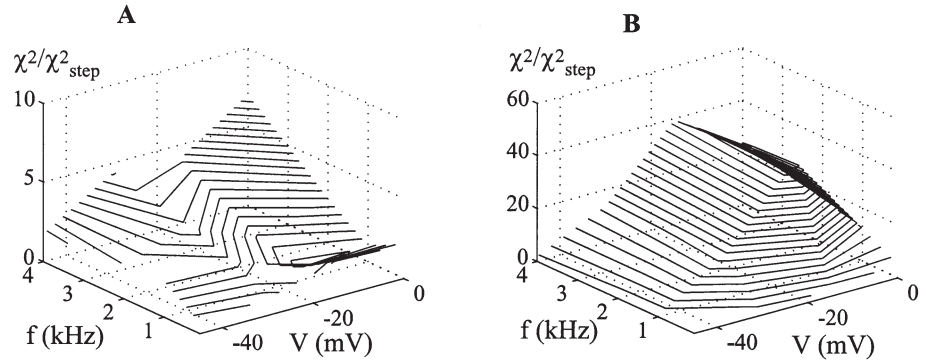

Figure 10. Model fit to experimental data for a range of sine voltage inputs of amplitude 45 mV, frequency between 0 and 4 kHz and mean values from 0 to −45 mV. The model fit computed as χ^2 is normalized to the fit of each model to activation transient and tail currents. A. Model A. Fit to experimental data remains of the same order of magnitude for a large range of voltage inputs. B. Model B. The model fit becomes progressively worse for higher frequency voltage inputs (>0.5 kHz). For voltage mean value of about −15 mV, the model fit is up to 45 times worse than for stepped-voltage protocols. For model D. (not shown) the fit is about 20 times worse for oscillating voltage inputs.

Discussion

One of the goals in studies of ion channels is to understand the channel gating kinetics, i.e. to develop a theoretical model that would summarize collected experi-

mental data. Thee most common type of models used for voltage gated ion channels are Markov models consisting of a number of discrete configurational states of the channel molecules and thermally activated transitions between the states. Deciding on the number of the states and their interrelation (the model topology) as well as finding transition rates between the states is the main goal of ion channel modelers. Unfortunately, while selecting *a* model for ion channel is relatively easy, choosing *the best* model is far more difficult. Typically there are many models, differing in their topology and their parameters, that are capable of reproducing experimental data equally well. It has been argued that this modeling ambiguity is inherent to the type of experimental techniques applied. All known voltage clamp protocols use only a finite number of voltage steps for all types of recordings: ionic, gating and single-channel. This means that the system under study (the ensemble of ion channels) is always at or near the state of equilibrium. Even if we add more and more of such experimental protocols they do not put essentially new constraints on the models for a given channel since they all belong to the same class of what we call *stepped-voltage* protocols.

In this paper we explore further the idea of driving ion channels far from equilibrium by fast varying voltages with the aim of exploring new aspects of channel kinetics that might be "unseen" by standard methods. Previously a number of random dichotomous noise voltages has been applied to hH1k sodium channels expressed in HEK293 cells (Millonas and Hanck 1998a,b). We explored another possibility of applying sinusoidal voltages of various mean values, amplitudes and frequencies. One might expect that this is not the optimal choice; stochastic signals might be more useful for this purpose (Bendat and Piersol 2000) and numerical results on using various random potentials have been reported (Kargol et al. 2002). In this paper we report our first and simplest NRS protocol, for which a comparison of model and experimental data is particularly simple. As a test case we chose the Shaker potassium channel, for which a variety of models were proposed by different research groups. In particular we concentrated here on models proposed in (Zagotta et al. 1994a). The four ZHA models were originally evaluated for their ability to reproduce a variety of steady state and kinetic data obtained, including both the whole cell and single channel data. Model D was selected as the best, although it was admitted that there were certain properties of channel kinetics that it did not describe well.

In this paper we reevaluated the ZHA models using the oscillating potentials. Since models cannot be proved, but only disproved, we set out to disprove some of the ZHA models by imposing new constraint stemming from new sets of data to be reproduced. Our main goal was to choose among various topologies, rather than to compare model parameters. To that end we performed standard experiments with the typical activation and tail series' and found that ZHA models A, B and D performed almost equally well in describing this data. As we already mentioned the models were originally developed to fit single channel data as well and although we do not present a direct comparison here, these models do pass the single channel data test as reported in (Zagotta et al. 1994a). Model C which fit well the steady-

state data failed with the activation kinetics and was therefore discarded based on the standard protocols alone. As we argue we found the three remaining models (A, B, and D) consistent with the experimental data and the differences between model currents were of the same order or smaller than the fitting accuracy of each model to the experimental currents. In other words we found no way to choose the best of the three based on the activation and tail series' alone.

We found, however, that oscillating voltages can offer a method for selecting the most appropriate model. As shown, the difference in model currents depends quite significantly on the frequency and mean value of the applied sinusoidal voltage. One can notice that for frequencies larger than 1 kHz and in the appropriate voltage range (generally for mean values within the channel activation range, as determined from the activation series) there are marked differences in both the steady-state current amplitudes and their time course. These differences as shown in Fig. 9A,B, far exceed the fitting accuracy of each model. A direct comparison with the experimental data shows that while for small frequencies (e.g. 0.1 kHz) the models perform equally well as for the stepped-voltage protocols, for frequencies above the threshold of 0.5–1 kHz models' B and D fit becomes progressively worse. On the other hand model A, which in case of stepped-voltage protocols was the worst, shows an excellent fit, at least for more depolarized voltages. On possible explanation would be that while the full kinetic scheme for the channel might be the one shown by model D, when fast oscillating voltages are applied the channel becomes "trapped" in a subset of the overall set of states, in this case allowing only transitions between states R_2 and A in kinetic scheme D. Such reduced model is the same as model A. How to incorporate this "trapping" mechanism into the kinetic scheme or what might be the physical mechanisms behind it, if indeed it is what happens, is uncertain.

We showed that the model proposed by in (Zagotta et al. 1994a) as a final result of their exhaustive study in fact has limited applicability. That clearly suggests that there are aspects of channel kinetics that become apparent only under nonequilibrium forcing and have not been taken into account in previous modeling efforts. It is a known fact exploited in other studies (Menconi et al. 1998; Xie et al. 1997; Liu et al. 1990) that new phenomena can be observed in biological macromolecules driven by periodic forces. It warrants in our opinion further study of the NRS technique. The example of NRS protocols used in Millonas and Hanck (1998a,b), Hosein-Sooklal and Kargol (2002) and the protocols used in this paper belong to two very different classes – random *vs.* regular. Of course there are infinitely many different waveforms that could be applied and the question of choosing the protocols most effective for a give channel has been addressed elsewhere (Kargol et al. 2002).

Acknowledgements. The authors would like to thank Prof. Mark M. Millonas for his inspiration and suggestions that led to this project.

References

Ball F. G., Rice J. A. (1992): Stochastic models for ion channel: Introduction and bibliography. Math. Biosci. **112**, 189—206

Bendat J. S., Piersol A. G. (2000): Random data: analysis and measurement procedures. Wiley, New York

Bezanilla F. (2002): Voltage sensor movements. J. Gen. Physiol. **120**, 465—473

Bezanilla F., Armstrong C. M. (1977): Inactivation of the sodium channel. I. Sodium current experiments. J. Gen. Physiol. **70**, 549—566

Cha A., Snyder G. E., Selvin P. R., Bezanilla F. (1999): Atomic scale movement of the voltage-sensing region in a potassium channel measured *via* spectroscopy. Nature **402**, 809—816

Eyring H. (1935): The activated complex in chemical reactions. J. Chem. Phys. **3**, 107—115

Fohlmeister J. F., Adelman W. J. Jr. (1985a): Gating current harmonics. I. Sodium channel activation in dynamics steady states. Biophys. J. **48**, 375—390

Fohlmeister J. F., Adelman W. J. Jr. (1985b): Gating current harmonics. II. Model simulation of axonal gating currents. Biophys. J. **48**, 391—400

Fohlmeister J. F., Adelman W. J. Jr. (1986): Gating current harmonics. III. Dynamic transients and steady states with intact sodium inactivation Biophys. J. **50**, 489—502

Fohlmeister J. F., Adelman W. J. Jr. (1987): Gating current harmonics. IV. Dynamic properties of secondary activation kinetics in sodium channel gating. Biophys. J. **51**, 335—338

Gandhi C. S., Isacoff E. Y. (2002): Molecular models of voltage sensing. J. Gen. Physiol. **120**, 455—463

Glauner K. S., Mannuzzu L. M., Gandhi C. S., Isacoff E. Y. (1999): Spectroscopic mapping of voltage sensor movement in the Shaker potassium channel. Nature **402**, 813—817

Hille B. (1992): Ionic channels of excitable membranes. Sinauer Associates Inc., Sunderland Massachussetts

Hoshi T., Zagotta W. N., Aldrich R. W. (1994): Shaker potassium channel gating I: Transition near the open state. J. Gen. Physiol. **103**, 249—278

Hosein-Sooklal A., Kargol A. (2002): Wavelet analysis of nonequilibrium ionic currents in human heart sodium channel (hH1a). J. Membrane Biol. **188**, 199—212

Jiang Y., Lee A., Chen J., Ruta V., Cadene M., Chait B. T., MacKinnon R. (2003a): X-ray structure of a voltage-dependent K^+ channel. Nature **423**, 33—41

Jiang Y., Ruta V., Chen J., Lee A., MacKinnon R. (2003b): The principle of gating charge movement in a voltage-dependent K^+ channel. Nature **423**, 42—48

Kargol A., Smith B., Millonas M. M. (2002): Application of nonequilibrium response spectroscopy to the study of channel gating. J. Theor. Biol. **218**, 239—258

Kienker P. (1989): Equivalence of aggregated Markov models of ion-channel gating. Proc. R. Soc. London, Ser. B **236**, 269—309

Korn S. J., Horn R. (1988): Statistical discrimination of fractal and Markov models of single channel gating. Biophys. J. **54**, 871—877

Larsson H. P. (2003): The search is on for the voltage sensor-to-gate coupling. J. Gen. Physiol. **120**, 475—481

Levitt D. G. (1989): Continuum model of voltage-dependent gating. Biophys. J. **55**, 489—498

Liebovitch L. S., Fischbarg J., Koniarek J. P. (1987): Ion channel kinetics. A model based on fractal scaling rather than Markov processes. Math. Biosci. **84**, 37—68

Liu D., Astumian R. D., Tsong T. Y. (1990): Activation of Na^+ and K^+ pumping modes of (Na,K)-ATPase by an oscillating electric field. J. Biol. Chem. **265**, 7260—7267

McManus O. B., Weiss D. S., Spivak C. E., Blatz A. L., Magleby K. (1988): Fractal models are inadequate for the kinetics of four different ion channels. Biophys. J. **54**, 859—870

Menconi M. C., Pellegrini M., Pellegrino M., Petracchi D. (1998): Periodic forcing of single ion channel: dynamic aspects of the open-closed switching. Eur. Biophys. J. **27**, 299—304

Millonas M. M. (2000): The micro-conformation approach to channel gating and its application the very early evens in shaker K+ channel activation. Biophys. J. **70**, 40Plat.

Millonas M. M., Hanck D. A. (1998a): Nonequilibrium response spectroscopy of voltage-sensitive ion channel gating. Biophys. J. **74**, 210—229

Millonas M. M., Hanck D. A. (1998b): Nonequilibrium response spectroscopy and the molecular kinetics of proteins. Phys. Rev. Lett. **80**, 401—404

Sakmann B., Neher E. (1995): Single-Channel Recording. (Eds. B. Sakmann and E. Neher), Plenum Press, New York—London

Sansom M. S. P., Ball F. G., Kerry C. J., McGee R., Ramsey R. L., Usherwood N. R. (1989): Markov, fractal, diffusion and related models of ion channel gating. Biophys. J. **56**, 1229—1243

Schoppa N. E., Sigworth F. J. (1998a): Activation of Shaker potassium channels. I. Characterization of voltage-dependent transitions. J. Gen. Physiol. **111**, 271—294

Schoppa N. E., Sigworth F. J. (1998b): Activation of Shaker potassium channels. II. Kinetics of the V2 mutant channel. J. Gen. Physiol. **111**, 295—311

Schoppa N. E., Sigworth F. J. (1998c): Activation of Shaker potassium channels. III. An activation gating model for wild-type and V2 mutant channels. J. Gen. Physiol. **111**, 313—342

Vandenberg C. A., Bezanilla F. (1991a): Single channel, macroscopic ionic, and gating currents in the squid giant axon. Biophys. J. **60**, 1499—1510

Vandenberg C. A., Bezanilla F. (1991b): A sodium channel gating model based on single channel, macroscopic ionic, and gating currents in the squid giant axon. Biophys. J. **60**, 1511—1533

Wagner M., Timmer J. (2000): Model selection in non-nested hidden Markov models for ion channel gating. J. Theor. Biol. **208**, 439—450

Xie T. D., Chen Y., Marszalek P., Tsong T. Y. (1997): Fluctuation-driven directional flow in biochemical cycle: further study of electric activation of Na,K pumps. Biophys. J. **72**, 2496—2502

Zagotta W. N., Hoshi T., Aldrich R. W. (1994a): Shaker potassium channel gating. III. Evaluation of kinetic models for activation. J. Gen. Physiol. **103**, 321—362

Zagotta W. N., Hoshi T., Dittman, J., Aldrich R. W. (1994b): Shaker potassium channel gating. II. Transitions in the activation pathway. J. Gen. Physiol. **103**, 279—319

Final version accepted: December 4, 2003